J|A|C|S
ARTICLES
Published on Web 01/31/2002

Oxygen as a Paramagnetic Probe of Membrane Protein Structure by Cysteine Mutagenesis and ^{19}F NMR Spectroscopy

Paul A. Luchette,[†] R. Scott Prosser,*[,†] and Charles R. Sanders[‡]

Contribution from the Department of Chemistry, Kent State University, Kent, Ohio 44242, and Department of Physiology and Biophysics, Case Western Reserve University, Cleveland, Ohio 44106-4970

Received August 1, 2001

Abstract: Oxygen solubility increases toward the hydrophobic interior of membranes. Using NMR, this O_2 solubility gradient gives rise to an exquisite range of position-dependent paramagnetic effects at partial pressures of 100 atm (PO_2), which may be used to probe membrane protein structure and positioning. In this study, fluorinated probes were introduced at selected positions of the transmembrane 1 domain of the intact homotrimer of the integral membrane protein, diacylglycerol kinase. Using ^{19}F NMR, O_2-induced chemical shift perturbations revealed secondary structure, membrane immersion depth, and regions of the helix in contact with the protein or with the micelle.

Membrane proteins, which represent 20−25% of all proteins, are central to photosynthesis and electron transfer, signal transduction, ion and molecular transport, and membrane-mediated catalysis.[1] Structure determination of this important class of protein is severely hampered by difficulties with the preparation of diffractable crystals, while high-resolution (TROSY) NMR studies of membrane proteins have thus far only been successful with β-based proteins.[2−4] A novel NMR approach, which utilizes oxygen as a paramagnetic reporter of membrane protein topology, is presented. Oxygen is inhomogeneously distributed in membranes and thus gives rise to an exquisite range of position-dependent paramagnetic effects at partial pressures of 100 atm (PO_2). In this study, fluorinated probes were introduced at selected positions of the transmembrane 1 (TM1) domain of the intact homotrimer of the integral membrane protein, diacylglycerol kinase (DAGK). Using ^{19}F NMR, O_2-induced chemical shift perturbations revealed secondary structure, membrane immersion depth, and regions of the helix in contact with the protein or with the micelle.

Fluorine NMR and the Paramagnetic Effect of Oxygen in Membranes. Fluorine which has a particularly sensitive nuclear spin for NMR studies is not found in native biological membranes and exhibits a chemical shift dispersion that is nearly 100 times that of ^1H NMR.[5] Through cysteine mutagenesis, and subsequent chemical derivatization, ^{19}F nuclei may be introduced at desired residue positions in membrane proteins. ^{19}F NMR chemical shifts are sensitive to local electrostatic and van der Waals environments, and the effect of paramagnetic agents is often dramatic.[6] Thus, water-soluble paramagnetic species such as Eu^{3+}, Dy^{3+}, or Yb^{3+}, or membrane-soluble species such as O_2, may be used in principle to determine the approximate membrane immersion depth and degree to which fluorine labels are exposed to water or buried in a membrane protein.

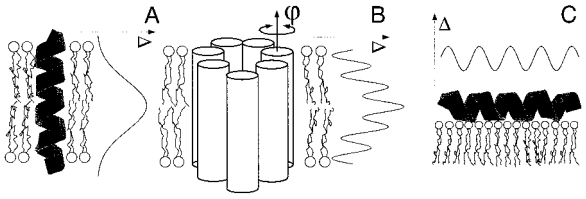

Figure 1. The effect of paramagnetic oxygen on ESR or NMR resonances along a transmembrane helix that exists either as a monomer (A) or as part of a larger aggregate (B). The Δ might represent a transverse relaxation rate or line width, or, as discussed in the text, a longitudinal paramagnetic relaxation rate. The φ relates to the degree of contact of the helix with the micelle hydrocarbon domain, as discussed in the text. In (B), a transmembrane helix is portrayed as being in contact with two neighboring helices, in which case a modulation of the paramagnetic effect through the bilayer is expected. In the case of an amphiphilic peptide (C), the paramagnetic profile is sinusoidal, though not modulated by immersion depth.

The concept of probing immersion depth and topology of membrane proteins by oxygen is illustrated in Figure 1 for both a transmembrane helix, that exists either as a monomer or as part of a complex, and a surface associated helix. In Figure 1A, the single transmembrane helix is expected to exhibit the greatest paramagnetic effects in the middle of the bilayer (as shown by the adjacent curve), since the oxygen concentration increases toward the hydrophobic interior of a bilayer.[7] In ESR, the O_2 paramagnetic effect (Δ) is collision-mediated (Heisenberg

* To whom correspondence should be addressed.
[†] Kent State University.
[‡] Case Western Reserve University.

(1) Popot, J. L.; Engelman, D. *Annu. Rev. Biochem.* **2000**, *69*, 881−922.
(2) Riek, R.; Wider, G.; Pervushin, K.; Wuthrich, K. *Proc. Natl. Acad. Sci. U.S.A.* **1999**, *96*, 4918−4923.
(3) Fernandez, C.; Adeishvili, K.; Wuthrich, K. *Proc. Natl. Acad. Sci. U.S.A.* **2001**, *98*, 2358−2363.
(4) Arora, A.; Abildgaard, F.; Bushweller, J. H.; Tamm, L. K. *Nat. Struct. Biol.* **2001**, *8*, 334−338.
(5) Gerig, J. T. *Prog. Nucl. Magn. Reson. Spectrosc.* **1994**, *26*, 293−370.
(6) Lau, E. Y.; Gerig, J. T. *J. Am. Chem. Soc.* **2000**, *122*, 4408−4417.

10.1021/ja016748e CCC: $22.00

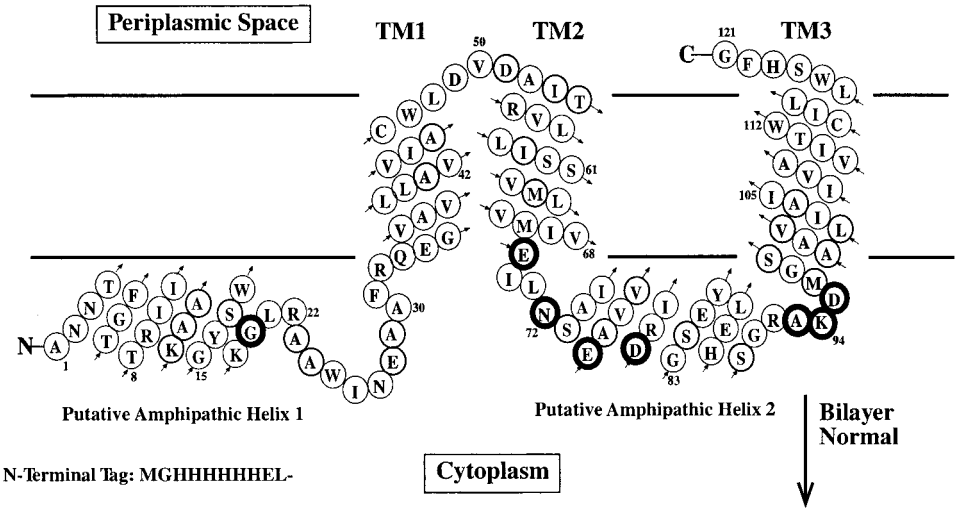

Figure 2. Model for wild type DAGK's membrane topology. Bold residues are those which are absolutely conserved in the approximately 30 available sequences for the prokaryotic enzyme (unpublished). While the locations of DAGK's three transmembrane domains are known on the basis of experimental data,[9] and DAGK is known to be a highly helical protein,[10] the exact secondary structure, beginnings, and ends of its transmembrane segments are not known, and the surface amphipathic helices are only putative, being predicted by sequence analysis. DAGK is known to function as a homotrimer,[11] in which TM2 lies at the central 3-fold axis of symmetry.[12]

exchange) and affects both saturation decay rates and line widths,[8] whereas in NMR, the paramagnetic interactions are manifested as changes in line widths, chemical shifts, and spin−lattice relaxation rates. If the helix is in contact with adjoining helices, as shown in Figure 1B, oxygen accessibility is determined both by depth and by the degree of exposure of the side chain to protein and hydrocarbon interfaces. The period of the oscillation directly relates to the number of residues per turn, which characterizes the helix. Finally, in the case of an amphipathic helix (1C), a flat oscillation of paramagnetic effects would be expected for either oxygen or some water-soluble paramagnetic agent. The phases of the two oscillation patterns would differ by 180° if one paramagnetic agent was membrane soluble and the other was water soluble.

DAGK as a Test Protein for Cysteine Mutagenesis and Paramagnetic Probing with Oxygen. Diacylglycerol kinase is a 39 kDa homotrimeric membrane protein, each subunit of which contains three transmembrane segments which are thought to be helices, as shown schematically in Figure 2.[9,10] Wild type DAGK possesses two cysteine residues. These residues were conservatively mutated to alanine, without loss of stability or protein activity.[13] A single-cysteine library with cysteine replacement mutants representing most sites of DAGK is available.[12,14] Most of these mutants exhibit catalytic activities approaching that of the wild type protein when properly purified and refolded.[14] For this study, available single-cys mutations for the first transmembrane segment (TM1) of the enzyme were purified, cys-thioalkylated with 3-bromo-1,1,1-trifluoropropanone, and subjected to a refolding/bilayer reconstitution procedure[14] yielding vesicular protein which was then redissolved with detergent to form mixed micelles in which DAGK is fully functional. Samples were then equilibrated at 100 atm (P_{O_2}) and subjected to NMR.

Results and Discussion

This study focused on residues 32−48, representing the first transmembrane segment of DAGK, which is suspected to lie on the outside of the homotrimer and would thus be in partial contact with the hydrophobic micelle interior.[12] One-dimensional ^{19}F NMR spectra, as shown in Figure 3B, were acquired with sufficient signal-to-noise after roughly 200 scans (10 min). Figure 3B also shows the effect of the addition of oxygen on the ^{19}F spectrum at a partial pressure of 100 atm. The most downfield peak in each spectrum represents a trace amount of trifluoroacetic acid (TFA) which was used as a reference. Although oxygen also shifts the reference, the (relative) 100 atm oxygen-induced shifts of the DAGK peaks are measured after overlaying the TFA reference peaks. A significant shift of the DAGK resonance, relative to that of TFA, is observed upon introduction of oxygen. The difference between this oxygen-induced shift and that observed at ambient oxygen partial pressures is plotted for each residue studied in the TM1 domain, as shown in Figure 3A. The chemical shift difference between the TFA reference and the respective DAGK resonance at ambient oxygen concentrations is also shown in Figure 3A. Though no obvious trend is observed for the chemical shift profile at ambient oxygen concentrations, a prominent oscillation with a periodicity of 3.6 residues is observed in the oxygen-induced shift profile. This trend is consistent with the shifts expected for a TM1 transmembrane α helix, which is thought to lie on the outside of the homotrimer complex. The chemical shift profile also displays an underlying Gaussian function, with a maximum near residue 40. This is interpreted to reflect the immersion depth effect (i.e., residue 40 is expected to be the central-most transmembrane residue). The above paramagnetic shift profile can be fitted to a function, Δ, which reflects the

(7) Windrem, D. A.; Plachy, W. Z. *Biochim. Biophys. Acta* **1980**, *600*, 655−665.
(8) Altenbach, C.; Marti, T.; Khorana, H. G. *Science* **1990**, *248*, 1088−1092.
(9) Smith, R. L.; Otoole, J. F.; Maguire, M. E.; Sanders, C. R. *J. Bacteriol.* **1994**, *176*, 5459−5465.
(10) Sanders, C. R.; Czerski, L.; Vinogradova, O.; Badola, P.; Song, D.; Smith, S. O. *Biochemistry* **1996**, *35*, 8610−8618.
(11) Vinogradova, O.; Badola, P.; Czerski, L.; Sonnichsen, F. D.; Sanders, C. R. *Biophys. J.* **1997**, *72*, 2688−2701.
(12) Nagy, J. K.; Lau, F. W.; Bowie, J. U.; Sanders, C. R. *Biochemistry* **2000**, *39*, 4154−4164.
(13) Lau, F. W.; Nauli, S.; Zhou, Y.; Bowie, J. U. *J. Mol. Biol.* **1999**, *290*, 559−564.
(14) Gorzelle, B. M.; Nagy, J. K.; Oxenoid, K.; Lonzer, W. L.; Cafiso, D. S.; Sanders, C. R. *Biochemistry* **1999**, *38*, 16373−16382.

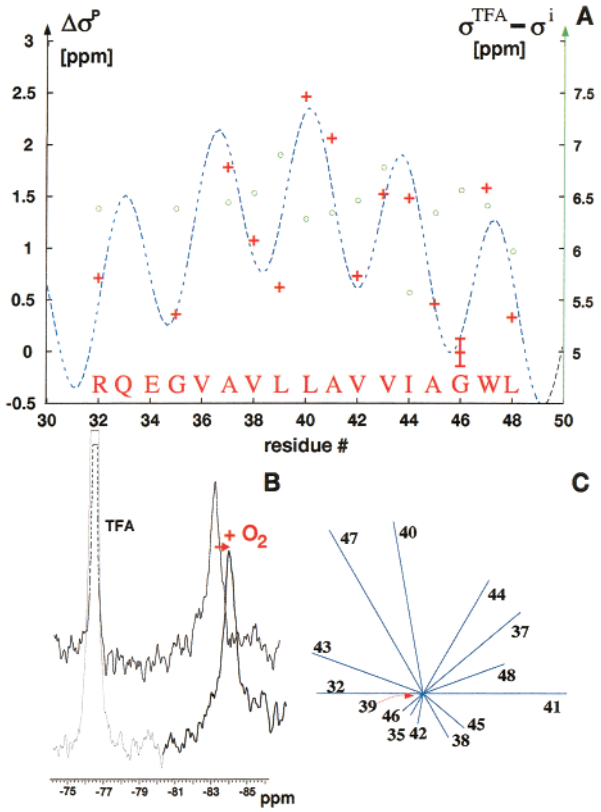

Figure 3. (A) One hundred atmospheres of oxygen-induced chemical shift changes (crosses) for ^{19}F-labeled single cysteine mutants from the TM1 domain of a membrane protein, DAGK, reconstituted into dodecylphosphocholine micelles, at 30 °C. Shifts were determined by measuring the change in the chemical shift difference from the reference (TFA at −76.55 ppm) and the peak maxima at 100 atm (P_{O_2}) and ambient oxygen partial pressure (0.2 atm). A typical approximation of uncertainty in estimation of the chemical shift perturbation, based on the line width, is shown for residue 46. The absolute chemical shift differences between TFA and the respective ^{19}F-labels at ambient oxygen concentrations are shown as diamonds. (B) Two characteristic spectra are shown for the mutant possessing a label at residue 39, both at 100 atm (P_{O_2}) and at 100 atm (P_{N_2}). The spectra were acquired on a Varian 500 Inova spectrometer at a Larmor frequency of 470.347 MHz, using 200 and 100 scans respectively, with a 2 s repetition time and a 5.2 μs $\pi/2$ pulse. The 5 mm (o.d.) sapphire NMR tube, designed to withstand nearly 200 atm, was fitted with a plug to prevent levitation of the liquid sample, resulting from the presence of O_2. Spectra were processed by an exponential apodization function with 50 Hz line broadening. (C) A helical wheel determined by subtracting the fitted depth-dependent chemical shift profile from the plotted profile (Figure 2A). Note that a value of 1.0 ppm was added to the magnitude of each vector so that they would all be portrayed as positive.

topological (sinusoidal) effect and the immersion depth (Gaussian) effect, such that

$$\Delta = A_1 \cos \frac{2\pi(n_{res} - n_0)}{3.6} + A_2 \exp\left[\frac{-(1.55(n_{res} - n_0))^2}{2\sigma^2}\right] \quad (1)$$

where n_{res} defines the residue number, and n_0 is a point in the middle of the transmembrane domain. The σ characterizes the width of the O_2 depth-dependent profile, while A_1 and A_2 govern the relative strength of the topological and immersion depth terms. Using a nonlinear least-squares fitting procedure, A_1 and A_2 were found to be 0.76 ± 0.12 and 0.79 ± 0.12 ppm, respectively. Because the local oxygen solubility depends sensitively on immersion depth,[15,16] higher pressures increase the depth-dependent effect (A_2). The width, σ, was fitted to a value of 5.1 ± 0.7 Å. A difference of widths (σ) for each of the TM segments would be expected to reflect a relative tilt between helices. Finally, n_0 was determined to be 40.2 ± 0.1, which relates directly to the overall phase, $2\pi n_0/3.6$ (or φ as shown in Figure 1). The local maxima of the sinusoidal profile correlate with the side of the helix facing the hydrophobic domain of the micelle. In the absence of tilt, we could describe the average immersion depth (with respect to the middle of the membrane) for each residue in the TM1 domain as $1.55|n_{res} - 40.2|$ Å, where n_{res} represents the residue number, as described above. Helical tilt can be easily incorporated into the analysis and is manifested both in terms of the envelope of the overall chemical shift profile and in terms of the effective width, σ. However, at this level of uncertainty of chemical shift changes, the effects of tilt can be ignored and are not considered in this paper.

The uncertainty in differential shifts is estimated on the basis of line widths, which are only marginally affected by oxygen. The relatively benign broadening effect of oxygen is largely due to its extremely short electronic relaxation time, which makes it an ideal paramagnetic probe for NMR. In contrast, the paramagnetic effects of oxygen are severe in ESR studies to the point where only ambient concentrations are feasible. Higher pressures and, consequently, larger concentration gradients translate into greater topological resolution and are only feasible in NMR studies. The effect of pressure is also of minor concern; below 250 atm, few structural or functional changes are in general observed.[17] Oxygen is small and uncharged and, therefore, relatively nonperturbing, while its concentration can be conveniently changed. Thus, it is straightforward to obtain spectra at ambient and moderate pressures and measure spectral changes arising from oxygen, using a single sample. The accuracy of such measurements on even larger membrane proteins will be compromised by larger line widths, resulting from increased tumbling times of the detergent protein aggregate. However, this may be compensated by introducing longer, more mobile reporter groups, while resolution may also benefit from ^{1}H decoupling and use of deuterated detergents or lipids. Through faster intramolecular motional averaging, modest spectral resolution and, thus, topological accuracy may be preserved even for large membrane proteins.

The above oxygen-induced chemical shift profile can also be interpreted in terms of a helical wheel diagram.[18] In this analysis, the fitted Gaussian profile is subtracted from the observed oxygen-induced chemical shift profile. In a perfect α helix, residues are placed at 100° intervals around the helix axis (i.e., 3.6 residues per turn), as shown in Figure 3C. The magnitude of each vector in this figure represents the degree of the shift perturbation and is maximal for residues which are in greatest contact with the micelle hydrocarbon domain. Note from the experimentally determined helical wheel that a 180° arc from the TM1 domain appears to be involved in contact with other protein domains.

The origin of the oxygen-induced shifts is not certain. Of the traditional paramagnetic interactions [contact shift and

(15) Prosser, R. S.; Luchette, P. A.; Westerman, P. W. *Biophys. J.* **2001**, *80*, 1406−1416.
(16) Prosser, R. S.; Luchette, P. A.; Westerman, P. W. *Proc. Natl. Acad. Sci. U.S.A.* **2000**, *97*, 9967−9971.
(17) Heremans, K.; Smeller, L. *Biochim. Biophys. Acta* **1998**, *1386*, 353−370.
(18) Schiffer, M.; Edmunson, A. B. *Biophys. J.* **1967**, *7*, 121.

pseudo-contact (dipolar) shift], the dipolar contribution would be expected to be negligible unless oxygen is somehow coordinated with the fluorinated label. However, large shifts of a contact nature have been observed in ^{13}C NMR studies of C_{60}, intercalated with molecular oxygen.[19,20] This contact shift, σ_{iso}, which is inversely proportional to temperature, T, and to the number of nearby oxygen molecules, n_{loc}, is given by

$$\sigma_{iso} = n_{loc}\left(\frac{A_{eff}}{\hbar}\right)\frac{g\mu_B S(S+1)}{3kT\gamma_I} \qquad (2)$$

where A_{eff} represents the motionally averaged hyperfine coupling constant, associated with the nuclei, of gyromagnetic ratio, γ_I ($g = 2$, and μ_B is a constant, while the electronic spin state, S, of oxygen is 1). Note that A_{eff}/γ_I is nearly the same for ^{13}C and ^{19}F nuclei, so that a significant contact shift in the presence of large local oxygen concentrations is possible. The magnitude of such shifts would depend on both the local oxygen concentration and the average residence time of the oxygen species.[20] At 100 atm, it has been estimated that the oxygen concentration may vary from 0.1 mM in the aqueous environment to more than 1 mM in the bilayer interior.[7,15] Consequently, a typical nuclear spin will on average be within a radius of roughly 12 Å of an oxygen molecule in the middle of the bilayer. This length is comparable to the average distance between the octahedral sites of the face-centered cubic lattice of C_{60} and the respective C_{60} nuclei.

Though the above results bear a qualitative similarity to the ESR results of others in studies of a variety of membrane proteins,[8] ^{19}F NMR offers several unique advantages. The nuclear spin label is less sterically and functionally perturbing than comparable nitroxide spin labels, while the short electronic relaxation time of oxygen permits the use of relatively high partial pressures and, consequently, large concentration gradients (and topological resolution) in the membrane. NMR line shapes and other spectroscopic indicators [Nuclear Overhauser Effects (NOEs) and spin−lattice relaxation rates] are easy to measure and interpret. For example, relatively long-range $^{19}F-^{19}F$ and $^{1}H-^{19}F$ distances can be probed by the measurement of specific NOEs.[21,22] Though NMR traditionally requires milligram quantities of protein samples, cryoprobe technology[23] and high magnetic fields[24,25] will soon improve sensitivity by more than an order of magnitude.

Though we have so far attributed the differential chemical shifts to local concentration gradients, differences in mobility may also contribute to the above shifts. Spin−lattice relaxation rate measurements, at ambient oxygen concentrations, are excellent independent measures of mobility, while polarity effects may be studied by contrasting the paramagnetic shift effects of oxygen with a water-soluble species such as europium. In ESR, polarity profiles, which typically involve the measurement of a ratio of a paramagnetic effect arising from water-soluble nickel to that from membrane-soluble oxygen at ambient pressure,[26] are often particularly sensitive to secondary structure, tilt, and topology. In the above study, spin−lattice relaxation rates (at ambient oxygen concentrations) revealed no significant variation in rates as a function of residue, leading us to rule out local mobility as a direct cause of paramagnetic shifts.

The above application of oxygen to probe structure and topology, through cysteine mutagenesis and ^{19}F NMR, indicates the usefulness of oxygen in studies of surfaces and as probes of local mobility. This has been recently demonstrated in the measurement of proton paramagnetic relaxation rates of a water-soluble protein, under low oxygen partial pressures.[27] The sensitivity of paramagnetic ^{1}H NMR relaxation rates, reported by Teng and Bryant for ribonuclease,[27] bodes well for the possibility of using oxygen to probe molecular accessibility and folding of water-soluble proteins.

Oxygen, as a paramagnetic probe, is not limited to ^{19}F NMR applications. Paramagnetic relaxation rates are proportional to the square of the gyromagnetic ratio and are thus expected to be significant for ^{1}H and ^{19}F, although large shifts and relaxation rates have been observed in recent ^{13}C (low gyromagnetic ratio) NMR studies, under similar conditions.[28] Thus, at moderate partial pressures, it should be possible to adapt many existing high-resolution NMR experiments to reveal O_2-induced ^{13}C chemical shift perturbations or ^{1}H spin−lattice relaxation rate changes to elucidate membrane protein topology. In this way, many direct applications of oxygen as a paramagnetic probe of topology can be envisioned for high-resolution ^{1}H NMR TROSY studies and solid-state NMR studies of membrane proteins.

Acknowledgment. R.S.P. gratefully acknowledges the support of Research Corporation (RIO322) and useful discussions with F. G. Walz, Jr., R. G. Bryant, P. W. Westerman, and E. Oldfield. C.R.S. acknowledges the support of NIH (R01 GM47485). We gratefully acknowledge Prof. J. Bowie (UCLA) for providing us with mutants for this study.

JA016748E

(19) Assink, R. A.; Schirber, J. E.; Loy, D. A.; Morosin, B.; Carlson, G. A. *J. Mater. Res.* **1992**, *7*, 2136−2143.
(20) Bernier, P.; Lukyanchuk, I. *Phys. Rev. B* **1996**, *53*, 7535−7538.
(21) Klein-Seetharaman, J.; Getmanova, E. V.; Loewen, M. C.; Reeves, P. J.; Khorana, H. G. *Proc. Natl. Acad. Sci. U.S.A.* **1999**, *96*, 13744−13749.
(22) Loewen, M. C.; Klein-Seetharaman, J.; Getmanova, E. V.; Reeves, P. J.; Schwalbe, H.; Khorana, H. G. *Proc. Natl. Acad. Sci. U.S.A.* **2001**, *98*, 4888−4892.
(23) Medek, A.; Olejniczak, E. T.; Meadows, R. P.; Fesik, S. W. *J. Biomol. NMR* **2000**, *18*, 229−238.
(24) Kiyoshi, T.; Sato, A.; Wada, H. *IEEE Trans. Appl. Supercon.* **1999**, *9*, 559−562.
(25) Markiewicz, W. D.; Schwartz, J.; Schneider-Muntau, H. J. *IEEE Trans. Appl. Supercon.* **2000**, *10*, 724−727.
(26) Hubbell, W. L.; Cafiso, D. S.; Altenbach, C. *Nat. Struct. Biol.* **2000**, *7*, 735−739.
(27) Teng, C. L.; Bryant, R. G. *J. Am. Chem. Soc.* **2000**, *122*, 2667−2668.
(28) Gangoda, M.; Prosser, R. S.; Luchette, P. A. 2001, unpublished results.